Gate-tunable weak antilocalization in a few-layer InSe

Junwen Zeng,[1] Shi-Jun Liang,[1] Anyuan Gao,[1] Yu Wang,[1] Chen Pan,[1] Chenchen Wu,[1] Erfu Liu,[1] Lili Zhang,[1] Tianjun Cao,[1] Xiaowei Liu,[1] Yajun Fu,[1] Yiping Wang,[1] Kenji Watanabe,[2] Takashi Taniguchi,[2] Haizhou Lu,[3] and Feng Miao[1,*]

[1]*National Laboratory of Solid State Microstructures, School of Physics, Collaborative Innovation Center of Advanced Microstructures, Nanjing University, Nanjing 210093, China*

[2]*National Institute for Materials Science, 1-1 Namiki Tsukuba, Ibaraki 305-0044, Japan*

[3]*Institute for Quantum Science and Engineering and Department of Physics, South University of Science and Technology of China, Shenzhen 518055, China*

(Received 30 April 2018; revised manuscript received 27 August 2018; published 18 September 2018; corrected 2 October 2018)

Indium selenide (InSe) has attracted tremendous research interest due to its high mobility and potential applications in next-generation electronics. However, the underlying transport mechanism of carriers in thin InSe at low temperatures remains unknown. Here we report the gate voltage and temperature-dependent magnetotransport properties of γ-InSe transistor devices with Hall mobility up to 2455 $\mathrm{cm^2\,V^{-1}\,s^{-1}}$ at the temperature of 1.7 K. We observe a gate-tunable weak antilocalization behavior at lower magnetic field B, which shows a transition to weak localization at higher B region. We find that the magnetotransport data agree well with the Hikami-Larkin-Nagaoka theory. The conductivity and temperature dependence of phase-coherence length reveal that the electron-electron (*e-e*) interactions are dominated dephasing mechanism for electronic transport in γ-InSe at low temperatures. The maximum phase-coherence length is found to be 320 nm at 1.7 K, larger than that of monolayer MoS_2 and few-layer black phosphorus. These results enrich the fundamental understanding of electronic transport properties of InSe.

DOI: 10.1103/PhysRevB.98.125414

I. INTRODUCTION

Conventional two-dimensional (2D) materials [1], such as graphene [2], transition-metal dichalcogenides (TMDs) [3], and black phosphorus [4], have been studied extensively over the last decade, not only for their fundamental physical properties [5–8], but also for their potential electronic, optical, and thermal applications [9,10]. Recently, layered-structure III-VI semiconductors have generated great interest among the scientific community, with their excellent electronic and optical properties [11–15]. One of the candidates among layered-structure III-VI semiconductors is indium selenide (InSe), which has been extensively studied in experiments [13–19]. Most experiments on studying InSe focused on utilizing its high photoresponsivity to explore optoelectronic applications [16,18,19]. The carrier transport properties of few-layer InSe have been rarely investigated. A most recent work has shown that the mobility of few-layer InSe encapsulated in hexagonal boron nitride (hBN) can be up to $10^4\,\mathrm{cm^2\,V^{-1}\,s^{-1}}$ at liquid-helium temperature [15]. The reported room-temperature mobility ($\sim$2000 $\mathrm{cm^2\,V^{-1}\,s^{-1}}$) of the thin InSe [15] is higher than that of silicon ($\sim$1000 $\mathrm{cm^2\,V^{-1}\,s^{-1}}$) [20], and much higher than that of few-layer 2D TMDs ($\sim$150 $\mathrm{cm^2\,V^{-1}\,s^{-1}}$) under the similar field-effect measurement [21], making 2D InSe an ideal electronic material for new-generation field-effect transistors (FET). Despite this significant progress, scattering mechanisms of electronic transport in few-layer InSe remain elusive.

Previous works have shown that studies of quantum interference corrections to conductivity in mesoscopic systems give a fundamental understanding of intrinsic carriers' transport properties [22,23]. For example, measurement of magnetoresistance is often regarded as an effective method to investigate the microscopic origin of scattering mechanisms of quantum decoherence in 2D materials [24–28]. The weak localization (WL) or weak antilocalization (WAL) phenomenon, determined by constructive or destructive interference between time-reversed paths, is expected to occur in the quantum diffusive transport regime and usually associated with scattering mechanisms.

In this work, we perform electrical transport measurements of few-layer γ-InSe at low temperatures. The gate voltage and temperature dependence of magnetoresistance was studied to reveal the specific electron dephasing mechanisms. The observed WAL effect indicates that spin-orbit interaction in γ-InSe induced by gate voltage plays a key role in the magnetotransport characteristics. The extracted phase-coherence length l_φ [based on the fitting using the Hikami-Larkin-Nagaoka (HLN) model] is 320 nm at 1.7 K, larger than that of monolayer MoS_2 [26] and few-layer black phosphorus [24,25]. Furthermore, l_φ exhibits a quasilinear dependence on conductivity, and is proportional to $T^{-0.5}$ for fixed gate voltage, indicating that the electron dephasing mechanism in γ-InSe originates from electron-electron interactions at low temperatures.

As a family member of III-VI group metal chalcogenides, γ-InSe is a van der Waals layered semiconductor with a layer-dependent band gap. Monolayer γ-InSe is composed of four atomic layers with Se-In-In-Se arrangement, which forms a honeycomb lattice [Fig. 1(a)] [15,29]. Figure 1(b) shows Raman spectra of the InSe sample used for the magnetotransport measurements. Four prominent peaks appear at 116.6, 176.7,

*miao@nju.edu.cn

 ©2018 American Physical Society

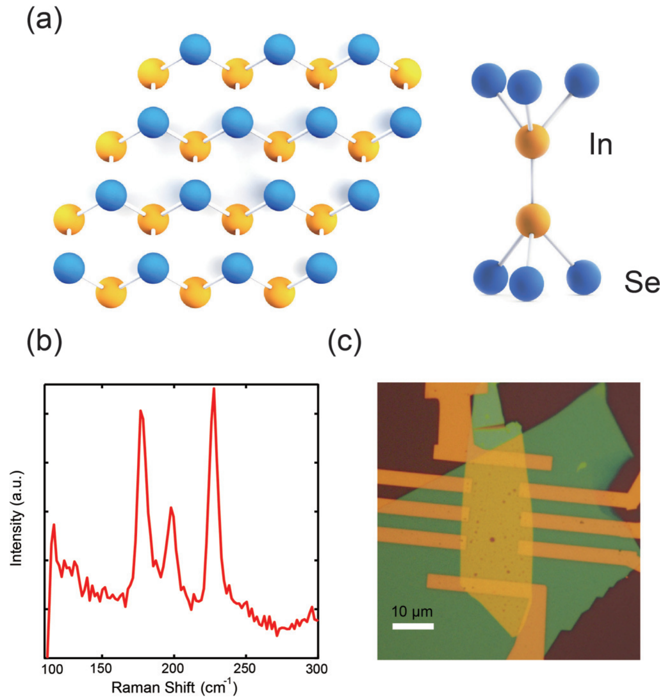

FIG. 1. γ-InSe/hBN devices. (a) Schematic of γ-InSe crystal structure. Left panel shows a honeycomb lattice in basal plane and right panel displays a bulk unit cell. (b) Raman spectra of the InSe device. (c) Optical image of a typical fabricated γ-InSe/hBN field-effect transistor device. The scale bar is 10 μm.

197.8, and 227.7 cm^{-1}, corresponding to $A_1^{'}(\Gamma_1^2)$, $E'(\Gamma_3^1) -$ TO and $E''(\Gamma_3^3)$, $A''(\Gamma_1^1) -$ LO, $A_1^{'}(\Gamma_1^3)$ modes, respectively, which is consistent with the previous works [16,30].

II. METHODS

To fabricate high-quality γ-InSe devices, we transfer mechanically foliated few-layer γ-InSe onto the insulating hBN substrate, which is produced by mechanical exfoliation onto Si wafers covered by 300-nm oxide. The entire process described above was carried out in a glove box filled with pure nitrogen to avoid undesirable contaminations or material reactions. Using standard electron-beam lithography (EBL) and electronic-beam evaporation of Ti/Au (5/50 nm) for metal electrodes, we fabricate the γ-InSe FET devices for electrical transport measurements in a He^4 cryostat. Before the step of cooling down, the devices were annealed in a pure argon atmosphere at a temperature of 270 °C for 3 h to remove polymer residues arising from the preceding EBL process, and to reduce contact resistance. Figure 1(c) shows an optical image of a typical γ-InSe FET device. To study the effect of hBN substrate on the mobility of InSe devices, we have measured the transfer curves of three different InSe/hBN devices and four different InSe/SiO_2 devices at room temperature. Figure 2(a) shows the two-terminal conductivity $\sigma_{2\mathrm{p}}$ [$\sigma_{2\mathrm{p}} = (L/W)(I_{\mathrm{ds}}/V_{\mathrm{ds}})$], where L, W is the length and width of the channel, respectively, I_{ds} is the drain-source current as a function of back-gate voltage V_{bg} under a drain-source bias voltage of 0.1 V for different devices, exhibiting a typical n-type behavior of InSe/hBN devices (red lines). Compared to the InSe/SiO_2 FET devices (blue lines), we find that the on-state current in InSe/hBN devices increases by over one order of magnitude. We calculate the corresponding field-effect mobility by the Drude model, [$\mu_{\mathrm{FE}} = \partial(\sigma)/\partial(C_{\mathrm{g}}V_{\mathrm{bg}})$, where C_{g} is the capacitance per unit area between the conducting channel and back gate]. The results are shown in Fig. 2(b) with a histogram plot. We can see that the mobility of InSe/SiO_2 devices is smaller than that of InSe/hBN devices. Thus the hBN substrate is an ideal candidate for InSe to improve the mobility.

III. RESULTS

By employing both two- and four-terminal resistance measurements, we study FET characteristics of InSe/hBN devices with temperatures ranging from 1.7 to 70 K (Fig. 3). Figure 3(a) shows the curves of $\sigma_{2\mathrm{p}}$ vs V_{bg} with $V_{\mathrm{ds}} = 0.1$ V. The variation of $\sigma_{2\mathrm{p}}$ with T may be due to the effect of Schottky barrier at the contacts, which is consistent with the previous

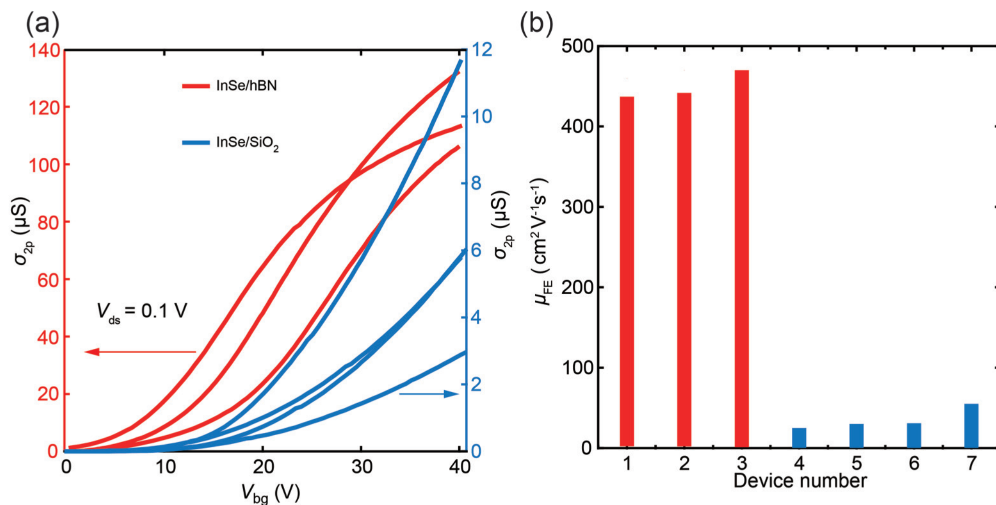

FIG. 2. (a) The conductivity $\sigma_{2\mathrm{p}}$ vs V_{bg} of three InSe/hBN devices (red lines) and four InSe/SiO_2 devices (blue lines). (b) The histogram of mobility of three InSe/hBN devices (red pillars) and four InSe/SiO_2 devices (blue pillars).

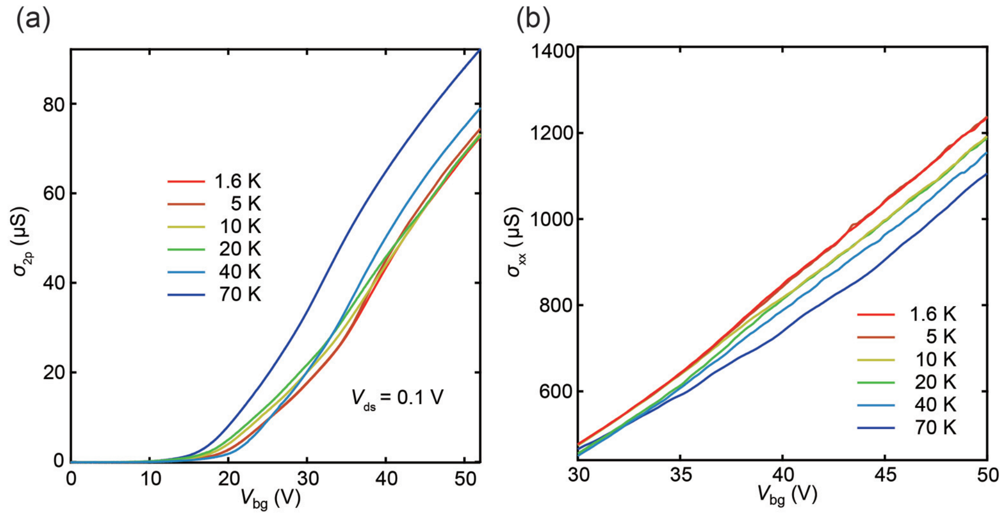

FIG. 3. Transfer curves at various temperatures. (a) Two-terminal conductivity σ_{2p} varies with back-gate voltage V_{bg}. (b) Four-terminal conductivity σ_{xx} as a function of V_{bg}.

report [14]. To eliminate the effect of contact resistance, we also conduct the measurements of four-terminal sheet resistance R_{xx} by an ac technique (with a Stanford Research 830 lock-in amplifier). The four-terminal conductivity [$\sigma_{xx} = (L/W)(1/R_{xx})$] as a function of V_{bg} is shown in Fig. 3(b). In contrast to the two-terminal measurements presented in Fig. 3(a), σ_{xx} increases as the temperature decreases, indicating the presence of metallic conduction of γ-InSe at the regime of $V_{bg} \geqslant 30\,\text{V}$. From the curves of σ_{xx} vs V_{bg}, we can extract the field effect mobility μ_{FE}, with the maximum value up to $3450\,\text{cm}^2\,\text{V}^{-1}\,\text{s}^{-1}$ at $T = 1.6\,\text{K}$ [Fig. 4(b)]. An effective dielectric screening from hBN substrate may account for the observed high field-effect mobility of the γ-InSe devices [15,31,32]. By carrying out the measurement of Hall effect [Fig. 4(a)], we can obtain the Hall mobility μ_H with the equation of $\mu_H = \sigma_{xx}/ne$ and $(n = 1/\text{e})\frac{dB}{dR_{xy}}$ (R_{xy} is the Hall resistance) [Fig. 4(b)]. μ_H increases with decreasing T and exhibits a maximum value of around $2455\,\text{cm}^2\ \text{V}^{-1}\,\text{s}^{-1}$ at $T = 1.6\,\text{K}$ and $V_{bg} = 50\,\text{V}$. The Hall mobility is less than the field-effect mobility due to an additional term resulted from the gate-dependent μ_H included in the field-effect mobility [$\mu_{FE} = \mu_H + (V_{bg} - V_{th})\frac{d\mu_H}{dV_{bg}}$, where V_{th} is the threshold voltage].

To further study the underlying quantum-scattering mechanisms in γ-InSe FET devices, we also examine gate-voltage dependence of magnetoresistance under a perpendicular magnetic field at temperature of 1.7 K. Because a quantum correction to the electrical transport of γ-InSe can be manifested in the WL or WAL effect, the variation in conductivity could reveal the inelastic scattering mechanisms. In Fig. 5(a), we plotted magnetoconductivity (MC) as a function of the applied magnetic field for different gate voltages ranging from 30 to 47.5 V. The MC is defined as $\Delta\sigma_{xx}(B) = \sigma_{xx}(B) - \sigma_{xx}(0)$, where $\sigma_{xx}(B) = (L/W)[1/R_{xx}(B)]$ (the absolute value of $\sigma_{xx}(B)$ shown in Supplemental Material Fig. S1 [33]), with $R_{xx}(B)$ being magnetic-field-dependent four-terminal

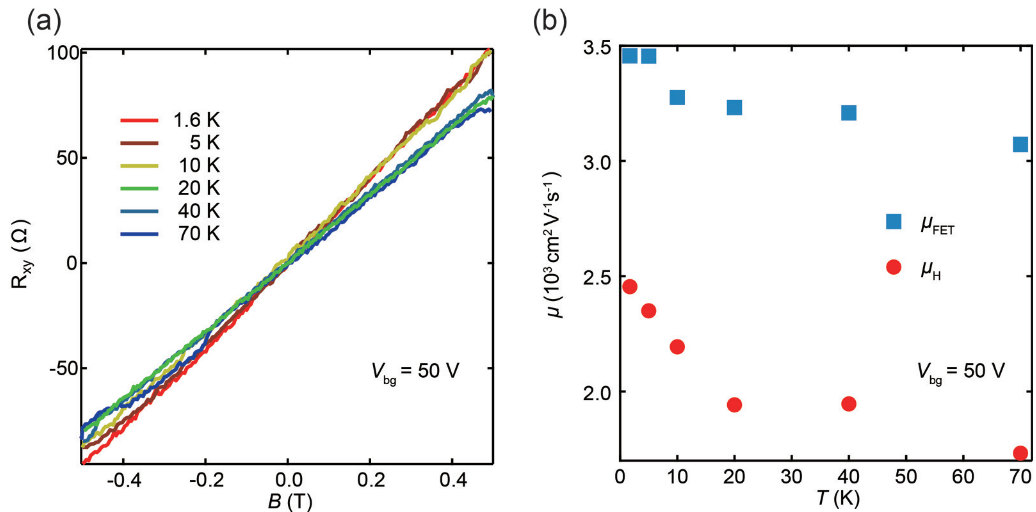

FIG. 4. (a) R_{xy} as a function of B at fixed gate voltage $V_{bg} = 50\,\text{V}$ and different temperatures between 1.6 and 70 K. (b) Temperature-dependent Hall and field-effect mobility.

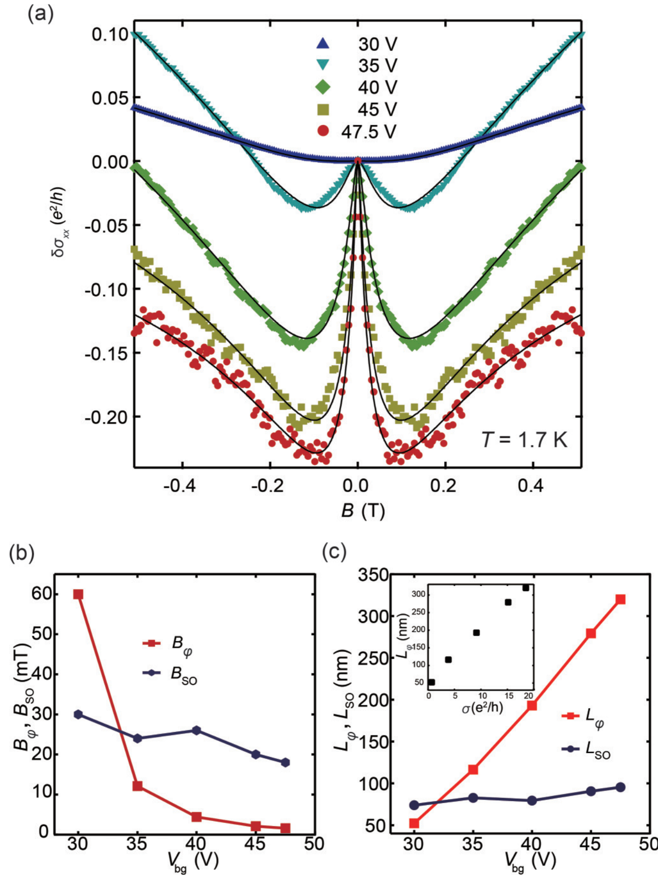

FIG. 5. Analysis of the gate-voltage-dependent magnetotransport of γ-InSe at $T = 1.7$ K. (a) $\Delta\sigma_{xx}$ as a function of magnetic field B at different gate voltages. The black solid lines are the fittings of the MC data with HLN model. (b) Gate-voltage-dependent characteristic field $B_{\varphi,}$ B_{SO} extracted from the fittings in (a). (c) The corresponding phase-coherence length l_φ and spin-orbit scattering length l_{SO} versus gate voltage.

resistance (similar to previous work [26,34], $R_{xx}(B)$ has been symmetrized to eliminate the contribution from Hall resistance: $R_{xx}(B) = \{[R_{xx}(-B) + R_{xx}(+B)]/2\}$). No significant change in $\Delta\sigma_{xx}(B)$ was detected at low magnetic field ($|B| \leqslant 0.13$ T) and low gate voltages ($V_{bg} \leqslant 30$ V). At larger V_{bg}, the $\Delta\sigma_{xx}(B)$ curves show a sharp cusplike feature with a peak at $B = 0$ T, which is a typical manifestation of the WAL effect. Additionally, we find that the amplitude of the drop in $\Delta\sigma_{xx}(B)$ increases with V_{bg}, and the conductivity also increases with V_{bg}, indicating that the WAL behavior is enhanced by conductivity [35]. At higher magnetic-field region, we find that MC increases with B for all the gate voltages, showing a crossover between the negative and positive magnetoconductivity. The similar phenomenon has been reported in the topological insulators [36]. Note that the band bending and disorder may also induce such a crossover. The band-bending effect can be negligible due to the weak bias voltage between source and drain ($V_{ds} = 0.1$ V). The disorder-induced transition from negative to positive magnetoconductivity generally occurs at the regime of lower carrier concentration (higher disorder strength) [37,38]. However the transition in Fig. 5(a) is observed in higher carrier concentration regime. Thus, the quantum interference effect is more reasonable to explain the crossover between the negative and positive magnetoconductivity. Note that the WAL effect is usually present in the materials with strong spin-orbit interaction (SOI) [26,39], and can also exist in the systems with a π Berry phase [40,41]. Recently, the WAL behavior has been also observed in GaSe, one of III-VI layered-structure compounds, and has been claimed to be dominantly determined by the Rashba SOI [42]. Since the previous experiments have demonstrated that the Berry phase is absent in 2D γ-InSe [15], the observed WAL effect is expected to be induced only by the SOI in γ-InSe, which will be discussed next.

We can gain further insights into the gate-voltage-dependent magnetotransport by fitting the $\Delta\sigma_{xx}(B)$ with the HLN theory [43–45]

$$\begin{aligned}\Delta\sigma_{xx}(B) = -\frac{e^2}{\pi h}\Bigg\{&\frac{1}{2}\left[\Psi\left(\frac{1}{2}+\frac{B_\varphi}{B}\right)-\ln\left(\frac{B_\varphi}{B}\right)\right]\\ &+\left[\Psi\left(\frac{1}{2}+\frac{B_{SO}+B_e}{B}\right)-\ln\left(\frac{B_{SO}+B_e}{B}\right)\right]\\ &-\frac{3}{2}\left[\Psi\left(\frac{1}{2}+\frac{\frac{4}{3}B_{SO}+B_\varphi}{B}\right)-\ln\left(\frac{\frac{4}{3}B_{SO}+B_\varphi}{B}\right)\right]\Bigg\},\end{aligned} \tag{1}$$

where e is the elementary charge, h is the Planck constant, Ψ is the digamma function. Here $B_i = h/(8\pi e l_i^2)$ ($i = \varphi$, SO, e) refers to the characteristic fields of phase coherence, spin-orbit, and elastic scattering, respectively, where l_i is the corresponding scattering length of each process ($l_i = \sqrt{D\tau_i}$, where D is the diffusion constant, and τ_i is the corresponding scattering time). B_e is introduced into the HLN model to study how the elastic scattering affects the magnetotransport of γ-InSe FET devices [44].

As can be seen in Fig. 5(a), the experimental results are in excellent agreement with the HLN theory for all the V_{bg}. Although $\sigma_{xx} < e^2/h$ occurs at $V_{bg} = 30$ V, the experimental data can be still well described by Eq. (1) similar to previous work [35]. This may be due to the fact that Fermi wavelength is less than the mean-free path (l), which can be justified by the estimation of $k_F l = 1.4$ (where k_F is Fermi momentum). Based on the fittings of HLN theory to the experimental data, we are able to extract the parameters (B_φ, B_{SO}), which are shown in Fig. 5(b) as a function of gate voltage for comparison. B_φ is found to decrease by one order of magnitude when increasing V_{bg} from 30 to 47.5 V. B_{SO} changes from 0.030 to 0.018 T, indicating that the spin-relaxation processes can be tuned by gate voltage. Furthermore, we investigate V_{bg} dependence of l_φ and l_{SO} at the temperature of 1.7 K, with results shown in Fig. 5(c). l_φ exhibits a superlinear dependence on V_{bg}, and reaches 320 nm at $V_{bg} = 47.5$ V; it is larger than that of monolayer MoS_2 [26] and few-layer black phosphorus [24,25] and comparable to that of graphene [27], which can be attributed to the small effective mass and the high mobility of γ-InSe. On the other hand, the spin-orbit scattering length l_{SO} slightly increases with V_{bg}, ranging from 74 nm at $V_{bg} = 30$ V to 96 nm at $V_{bg} = 47.5$ V. The V_{bg} weak dependence of l_{SO} may result from competition between the shortened spin-orbit scattering time τ_{SO} due to the gate-tuned Rashba SOI and

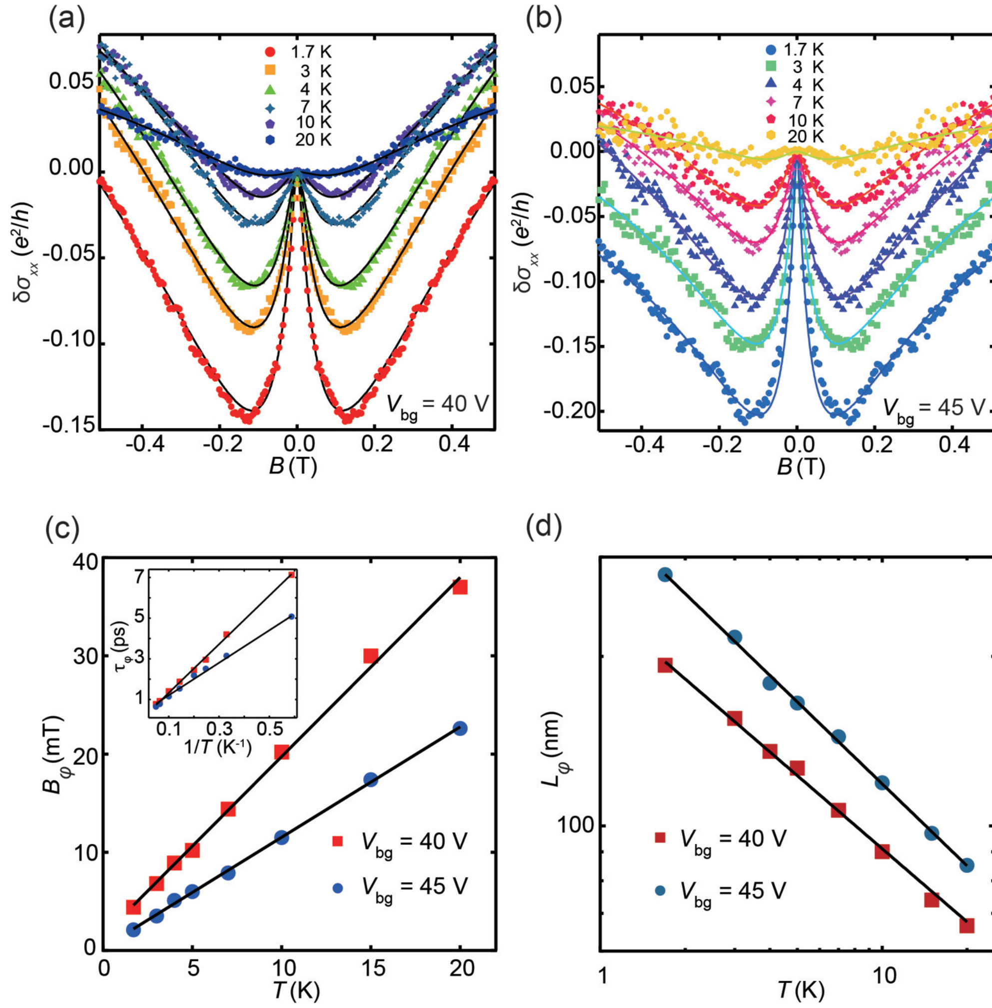

FIG. 6. Temperature-dependent phase-coherence length of γ-InSe. Fitting of the MC data with HLN model (the black solid lines) for $V_{\rm bg} = 40$ V (a) and 45 V (b). (c) Characteristic field B_φ estimated from the fitting with HLN model. The black solid lines are guides for the eye. The Inset shows curves of τ_φ vs T^{-1} for $V_{\rm bg} = 40$ and 45 V. (d) Phase-coherence length l_φ varies with temperatures, showing a power-law rule of $T^{-\gamma}$ (the black solid lines) with the $\gamma = 0.431 \pm 0.01$, $\gamma = 0.483 \pm 0.01$ for $V_{\rm bg} = 40$ and 45 V, respectively.

diffusion constant which increases with $V_{\rm bg}$ [Fig. 5(c)] ($D = v_F^2\tau_p/2$, where v_F is the Fermi velocity, τ_p is momentum scattering time). Usually, two primary factors in the quantum interference regime determine magnetoresistance behavior: phase coherence of electron and SOI-induced scattering. As shown in Fig. 5(c), the WAL effect occurs when coherence length l_φ is larger than SOI-induced scattering length $l_{\rm SO}$ [46]. As $V_{\rm bg}$ further increases, the WAL effect becomes more prominent with both Rashba SOI and l_φ increasing with $V_{\rm bg}$. The strength of spin-orbit interaction $\Delta_{\rm SO}$ can be estimated by using the relation of $\frac{2\hbar^2}{\tau_p\tau_{\rm SO}} = \Delta_{\rm SO}^2$. It increases from 1.1 meV at $V_{\rm bg} = 30$ V to 2.0 meV at $V_{\rm bg} = 47.5$ V, which is comparable to previous theoretical results of InSe in other phases [47] and the value for MoS_2 [26]. It is worthwhile to point out that the elastic scattering length l_e (15–40 nm) is one order of magnitude smaller than the inelastic phase-coherence length l_φ with the same $V_{\rm bg}$. In the regime of $l_e \ll l_\varphi$, a number of elastic collision events occur before an electron's phase is randomized. Thus the magnetotransport in γ-InSe FET devices at low temperatures is in the quantum diffusive regime. To further examine the effect of inelastic scattering on the carrier transport, l_φ is presented as a function of conductivity in the inset of Fig. 5(c). For *e-e* interactions, l_φ can be expressed as $l_\varphi = \frac{h\sigma_{\rm xx}}{4\pi\sigma_q}[\ln(\frac{\sigma_{\rm xx}}{\sigma_q})m^*k_BT]^{-1/2}$, where k_B is the Boltzmann constant [25,48]. The quasilinear conductivity dependence of l_φ is consistent with the *e-e* interactions mode at fixed temperature, implying that the main phase-relaxation mechanism at low temperatures is likely dominated by the *e-e* interactions. We will further discuss the origin of the dephasing scattering below.

IV. DISCUSSION

In general, two processes would give rise to the inelastic electron scattering at low temperatures: the *e-e* interactions with small energy transfer and the electron-phonon (*e*-ph) interactions [23,25]. To establish an understanding of the origin of inelastic dephasing scattering of electrons, we present the temperature-dependent magnetoresistance measurements with the same configuration of the magnetic field at fixed gate voltages. Figures 6(a) and 6(b) show $\Delta\sigma_{\rm xx}$ vs B at

various temperatures from 1.7 to 20 K for $V_{bg} = 40$ and 45 V, respectively. The sharp cusplike MC curves become flat as the temperature is increased. For temperatures above 20 K, the WAL effect disappears, due to the phase destruction resulting from increasing thermal fluctuations.

As expected, the HLN theory [Eq. (1)] also shows an excellent agreement with the experimental data in Figs. 6(a) and 6(b). The fittings enable the extraction of characteristic fields of phase coherence. In Fig. 6(c), we plot the characteristic field of phase coherence B_φ as a function of temperature for $V_{bg} = 40$ and 45 V, which displays a linear dependence. Furthermore, we utilize the relation of $\tau_\varphi = \hbar/(4eDB_\varphi)$ to obtain τ_φ at different temperatures from 1.7 to 70 K for $V_{bg} = 40$ and 45 V [see the inset of Fig. 6(c)]. We find that τ_φ is inversely proportional to T: $\tau_\varphi \propto T^{-1}$ at low temperatures, which is consistent with the theoretical estimation in Ref. [49]. To reveal the inelastic scattering mechanism, we show the temperature dependence of phase-coherence length l_φ [$l_\varphi = \sqrt{h/(8\pi eB_\varphi)}$] in Fig. 6(d) for $V_{bg} = 40$ and 45 V. Both cases exhibit $T^{-\gamma}$ dependence of l_φ over the entire studied temperature range, with $\gamma = 0.43 \pm 0.01$, $\gamma = 0.48 \pm 0.01$ for $V_{bg} = 40$ and 45 V. respectively. For carrier transport in 2D systems, both the *e-e* interactions and *e*-ph interactions can contribute to electron dephasing, and the corresponding γ for *e-e* (or *e*-ph) interactions is 0.5 (or 1) [23,25]. The measured values of γ are close to 0.5 for both gate voltages. Thus, we conclude that the *e-e* interaction with small energy transfer is the main mechanism, responsible for the phase relaxation in the quantum diffusive regime within temperatures ranging from 1.7 to 20 K. This conclusion is also consistent with the quasilinear trend of l_φ vs σ_{xx} [shown in Fig. 5(c)]. At lower temperatures, since other underlying dephasing mechanisms have been observed in certain 2D materials [26,50], they could also exist in thin γ-InSe, which is worth to be further explored in future work. Note that the magnetoresistance properties of InSe are different from that in topological insulator [51], in which the conventional HLN model has to be modified to include the *e-e* interactions to interpret the measured magnetoconductivity behavior.

V. CONCLUSION

In summary, we have observed the WAL effect in γ-InSe FET devices at low magnetic field, with a transition to WL at higher magnetic field. The observed WAL behaviors suggest that the SOI in γ-InSe tuned by gate voltage plays a key role in the magnetotransport characteristics at low-field region. By fitting the magnetotransport curves with the HLN model, a maximum phase-coherence length l_φ is found to be 320 nm at $T = 1.7$ K. Furthermore, we find a linear conductivity dependence of l_φ and a power-law temperature ($T^{-\gamma}$, with γ close to 0.5) dependence of l_φ, indicating that the *e-e* interactions are the dominant mechanism for electron dephasing in γ-InSe at low temperatures.

ACKNOWLEDGMENTS

This work was supported in part by the National Key Basic Research Program of China (2015CB921600, 2013CBA01603), the National Natural Science Foundation of China (61625402, 11374142, 61574076), and Fundamental Research Funds for the Central Universities and the Collaborative Innovation Center of Advanced Microstructures, Growth of hexagonal boron nitride crystals was supported by the Elemental Strategy Initiative conducted by the MEXT, Japan and JSPS KAKENHI Grant No. JP15K21722.

The authors declare no competing financial interests.

J.Z. and S.-J.L. are contributed equally to this work.

[1] A. K. Geim and I. V. Grigorieva, Nature (London) **499**, 419 (2013).

[2] K. S. Novoselov, A. K. Geim, S. V. Morozov, D. Jiang, Y. Zhang, S. V. Dubonos, I. V. Grigorieva, and A. A. Firsov, Science **306**, 666 (2004).

[3] B. Radisavljevic, A. Radenovic, J. Brivio, V. Giacometti, and A. Kis, Nat. Nanotechnol. **6**, 147 (2011).

[4] L. Li, Y. Yu, G. J. Ye, Q. Ge, X. Ou, H. Wu, D. Feng, X. H. Chen, and Y. Zhang, Nat. Nanotechnol. **9**, 372 (2014).

[5] K. Novoselov, A. K. Geim, S. Morozov, D. Jiang, M. K. I. Grigorieva, S. V. Dubonos, and A. A. Firsov, Nature (London) **438**, 197 (2005).

[6] Y. Zhang, Y. Tan, H. L. Stormer, and P. Kim, Nature (London) **438**, 201 (2005).

[7] E. Liu, Y. Fu, Y. Wang, Y. Feng, H. Liu, X. Wan, W. Zhou, B. Wang, L. Shao, and C. Ho, Nat. Commun. **6**, 6991 (2015).

[8] K. F. Mak, C. Lee, J. Hone, J. Shan, and T. F. Heinz, Phys. Rev. Lett. **105**, 136805 (2010).

[9] S. Z. Butler, S. M. Hollen, L. Cao, Y. Cui, J. A. Gupta, H. R. Gutierrez, T. F. Heinz, S. S. Hong, J. Huang, and A. F. Ismach, ACS Nano **7**, 2898 (2013).

[10] Q. H. Wang, K. Kalantar-Zadeh, A. Kis, J. N. Coleman, and M. S. Strano, Nat. Nanotechnol. **7**, 699 (2012).

[11] R. B. Jacobs-Gedrim, M. Shanmugam, N. Jain, C. A. Durcan, M. T. Murphy, T. M. Murray, R. J. Matyi, R. L. Moore, and B. Yu, ACS Nano **8**, 514 (2013).

[12] P. Hu, Z. Wen, L. Wang, P. Tan, and K. Xiao, ACS Nano **6**, 5988 (2012).

[13] W. Feng, W. Zheng, W. Cao, and P. Hu, Adv. Mater. **26**, 6587 (2014).

[14] S. Sucharitakul, N. J. Goble, U. R. Kumar, R. Sankar, Z. A. Bogorad, F. Chou, Y. Chen, and X. P. Gao, Nano Lett. **15**, 3815 (2015).

[15] D. A. Bandurin, A. V. Tyurnina, G. L. Yu, A. Mishchenko, V. Zólyomi, S. V. Morozov, R. K. Kumar, R. V. Gorbachev, Z. R. Kudrynskyi, S. Pezzini, Z. D. Kovalyuk, U. Zeitler, K. S. Novoselov, A. Patanè, L. Eaves, I. V. Grigorieva, V. I. Fal'ko, A. K. Geim, and Y. Cao, Nat. Nanotechnol. **12**, 223 (2017).

[16] S. Lei, L. Ge, S. Najmaei, A. George, R. Kappera, J. Lou, M. Chhowalla, H. Yamaguchi, G. Gupta, and R. Vajtai, ACS Nano **8**, 1263 (2014).

[17] G. W. Mudd, S. A. Svatek, T. Ren, A. Patane, O. Makarovsky, L. Eaves, P. H. Beton, Z. D. Kovalyuk, G. V. Lashkarev, and Z. R. Kudrynskyi, Adv. Mater. **25**, 5714 (2013).

[18] S. R. Tamalampudi, Y. Lu, R. Kumar U, R. Sankar, C. Liao, K. M. Boopathi, C. Cheng, F. C. Chou, and Y. Chen, Nano Lett. **14**, 2800 (2014).
[19] S. Lei, F. Wen, L. Ge, S. Najmaei, A. George, Y. Gong, W. Gao, Z. Jin, B. Li, and J. Lou, Nano Lett. **15**, 3048 (2015).
[20] N. D. Arora, J. R. Hauser, and D. J. Roulston, IEEE Trans. Electron Dev. **29**, 292 (1982).
[21] Z. Yu, Z. Ong, Y. Pan, Y. Cui, R. Xin, Y. Shi, B. Wang, Y. Wu, T. Chen, Y. Zhang, G. Zhang, and X. Wang, Adv. Mater. **28**, 547 (2016).
[22] B. L. Altshuler, D. Khmel'nitzkii, A. I. Larkin, and P. A. Lee, Phys. Rev. B **22**, 5142 (1980).
[23] C. Beenakker and H. van Houten, Solid State Phys. **44**, 1 (1991).
[24] Y. Du, A. T. Neal, H. Zhou, and D. Y. Peide, 2D Mater. **3**, 024003 (2016).
[25] Y. Shi, N. Gillgren, T. Espiritu, S. Tran, J. Yang, K. Watanabe, T. Taniguchi, and C. N. Lau, 2D Mater. **3**, 034003 (2016).
[26] H. Schmidt, I. Yudhistira, L. Chu, A. H. Castro Neto, B. Özyilmaz, S. Adam, and G. Eda, Phys. Rev. Lett. **116**, 046803 (2016).
[27] F. V. Tikhonenko, D. W. Horsell, R. V. Gorbachev, and A. K. Savchenko, Phys. Rev. Lett. **100**, 056802 (2008).
[28] E. McCann, K. Kechedzhi, V. I. Fal'ko, H. Suzuura, T. Ando, and B. L. Altshuler, Phys. Rev. Lett. **97**, 146805 (2006).
[29] P. Gomes da Costa, R. G. Dandrea, R. F. Wallis, and M. Balkanski, Phys. Rev. B **48**, 14135 (1993).
[30] J. F. Sánchez-Royo, G. Muñoz-Matutano, M. Brotons-Gisbert, J. P. Martínez-Pastor, A. Segura, A. Cantarero, R. Mata, J. Canet-Ferrer, G. Tobias, E. Canadell, J. Marqués-Hueso, and B. D. Gerardot, Nano Res. **7**, 1556 (2014).
[31] C. R. Dean, A. F. Young, I. Meric, C. Lee, L. Wang, S. Sorgenfrei, K. Watanabe, T. Taniguchi, P. Kim, and K. L. Shepard, Nat. Nanotechnol. **5**, 722 (2010).
[32] X. Cui, G. Lee, Y. D. Kim, G. Arefe, P. Y. Huang, C. Lee, D. A. Chenet, X. Zhang, L. Wang, F. Ye, F. Pizzocchero, B. S. Jessen, K. Watanabe, T. Taniguchi, D. A. Muller, T. Low, P. Kim, and J. Hone, Nat. Nanotechnol. **10**, 534 (2015).
[33] See Supplemental Material at http://link.aps.org/supplemental/10.1103/PhysRevB.98.125414 for the absolute value of conductivity as a function of magnetic field at different back gate voltage.
[34] S. Nakatsuji, N. Kiyohara, and T. Higo, Nature (London) **527**, 212 (2015).
[35] G. M. Minkov, A. V. Germanenko, and I. V. Gornyi, Phys. Rev. B **70**, 245423 (2004).
[36] H. Wang, H. Liu, C. Chang, H. Zuo, Y. Zhao, Y. Sun, Z. Xia, K. He, X. Ma, X. C. Xie, Q. Xue, and J. Wang, Sci. Rep. **4**, 5817 (2014).
[37] J. Liao, Y. Ou, X. Feng, S. Yang, C. Lin, W. Yang, K. Wu, K. He, X. Ma, Q. K. Xue, and Y. Li, Phys. Rev. Lett. **114**, 216601 (2015).
[38] P. M. Mensz and R. G. Wheeler, Phys. Rev. B **35**, 2844 (1987).
[39] J. B. Miller, D. M. Zumbühl, C. M. Marcus, Y. B. Lyanda-Geller, D. Goldhaber-Gordon, K. Campman, and A. C. Gossard, Phys. Rev. Lett. **90**, 076807 (2003).
[40] H. T. He, G. Wang, T. Zhang, I. K. Sou, G. K. L. Wong, J. N. Wang, H. Z. Lu, S. Q. Shen, and F. C. Zhang, Phys. Rev. Lett. **106**, 166805 (2011).
[41] F. V. Tikhonenko, A. A. Kozikov, A. K. Savchenko, and R. V. Gorbachev, Phys. Rev. Lett. **103**, 226801 (2009).
[42] S. Takasuna, J. Shiogai, S. Matsuzaka, M. Kohda, Y. Oyama, and J. Nitta, Phys. Rev. B **96**, 161303 (2017).
[43] W. L. Liu, M. L. Chen, X. X. Li, S. Dubey, T. Xiong, Z. M. Dai, J. Yin, W. L. Guo, J. L. Ma, and Y. N. Chen, 2D Mater. **4**, 011011 (2016).
[44] J. Hu, X. Liu, C. L. Yue, J. Y. Liu, H. W. Zhu, J. B. He, J. Wei, Z. Q. Mao, L. Y. Antipina, and Z. I. Popov, Nat. Phys. **11**, 471 (2015).
[45] S. Hikami, A. I. Larkin, and Y. Nagaoka, Prog. Theor. Phys. **63**, 707 (1980).
[46] H. Yuan, M. S. Bahramy, K. Morimoto, S. Wu, K. Nomura, B. Yang, H. Shimotani, R. Suzuki, M. Toh, C. Kloc, X. Xu, R. Arita, N. Nagaosa, and Y. Iwasa, Nat. Phys. **9**, 563 (2013).
[47] D. T. Do, S. D. Mahanti, and C. W. Lai, Sci. Rep. **5**, 17044 (2015).
[48] B. L. Altshuler, A. G. Aronov, and D. E. Khmelnitsky, J. Phys. C: Solid State Phys. **15**, 7367 (1982).
[49] B. N. Narozhny, G. Zala, and I. L. Aleiner, Phys. Rev. B **65**, 180202 (2002).
[50] S. Engels, B. Terrés, A. Epping, T. Khodkov, K. Watanabe, T. Taniguchi, B. Beschoten, and C. Stampfer, Phys. Rev. Lett. **113**, 126801 (2014).
[51] J. Wang, A. M. DaSilva, C. Z. Chang, K. He, J. K. Jain, N. Samarth, X. C. Ma, Q. K. Xue, and M. H. W. Chan, Phys. Rev. B **83**, 245438 (2011).

Correction: References [15] and [28] contained errors and have been corrected.